

## Spatiotemporal chaos from a continuous Na<sub>2</sub> laser

W. Klische and C. O. Weiss

*Physikalisch-Technische Bundesanstalt, Braunschweig, Federal Republic of Germany*

B. Wellegehausen

*Institut für Quantenoptik, Universität Hannover, Hannover, Federal Republic of Germany*

(Received 30 June 1988)

We report on the observation of spatiotemporal chaos in a multimode continuous Na<sub>2</sub> ring laser optically pumped by a single-mode Ar<sup>+</sup> laser. Measurements of the intensity of the emitted beam at two different points of the beam cross section reveal different temporal behavior of those two signals. Power spectra, fractal dimensions, and correlations indicate that both signals are chaotic and are generated by a common attractor.

While the study of temporal instabilities in lasers has received considerable interest for some time, it was only recently that these studies were extended to include spatial variations of the dynamics. In this Communication we report, to our knowledge, for the first time on the observation of spatiotemporal chaos in a laser.

We used the 525-nm Q13 laser transition of Na<sub>2</sub> pumped by a 488-nm single-mode Ar<sup>+</sup> laser to study the temporal behavior of the emitted intensity at two different points of the output beam simultaneously. This transition is known to have very high gain ( $0.2 \text{ cm}^{-1}$ ) with high-power pump lasers being available. Thus, the laser could be operated highly above threshold, which is generally known to favor instabilities. To reduce complicating effects standing-wave patterns in the laser were avoided by use of a ring resonator which also avoids unwanted feedback to the pump laser. While stable single-mode or multimode operation occurred for most of the parameter values, we also found chaotic multimode emission from this laser, which is described below.

The experimental setup is given in Fig. 1: The near confocal laser resonator consists of two highly reflecting spherical mirrors ( $r=200 \text{ mm}$ ) and a plane mirror with

10% transmission. A high-dispersion Brewster prism is used to select a single line from the Na<sub>2</sub> spectrum and to couple the pump power into the resonator. Additional losses from the Brewster windows, the prism, and from self-absorption of the radiation in the active medium are estimated to another 10%. The length of the ring is 350 mm, giving a cavity linewidth of 15 MHz. The active medium is sodium vapor at 770 K, contained in a heat pipe at a He buffer gas pressure of 3 Torr. The length of the vapor zone is 50 mm. To provide a high-gain-length product, there are two passes of the pump and laser beams through the heat pipe. Therefore, mirrors  $M_1$  and  $M_2$  are highly reflecting for the pump and the laser wavelengths.

The pump beam is matched to the fundamental mode of the resonator, giving a beam waist of 0.1 mm. The pump frequency is stabilized to an external Fabry-Pérot resonator, resulting in a laser linewidth of 500 kHz that is small compared to the homogeneous medium linewidth of 40 MHz (see below). The pump power was 300 mW, held constant within 0.3%. The intensity in the beam waist was  $10^3 \text{ W cm}^{-2}$  or 25 times the laser threshold pump intensity.

As a result of the dynamic Stark effect, the forward gain profile is split.<sup>1</sup> The splitting is estimated to be 30 MHz for the maximum intensity given above, while homogeneous line broadening is 40 MHz. Thus, the laser transition is in effect homogeneously broadened, which is well compatible with the high pump intensity necessary for the instabilities to occur. The natural linewidth is 22 MHz and the inhomogeneous Doppler linewidth is about 1.7 GHz (all linewidths are given as half width at half maximum in period frequencies). Due to the forward-backward gain asymmetry brought about by the Doppler effect, the Na<sub>2</sub> ring laser operates unidirectionally, the emitted beam propagating in the same direction as the pump beam.

For certain values of the resonator length, which served as the "control parameter" throughout the experiment, the Na<sub>2</sub> laser operated in the fundamental TEM<sub>00</sub> mode which yields maximum output power (10% of the pump power). For some other length values single-mode operation with higher-order transverse modes or stable multimode operation were observed. For intermediate length

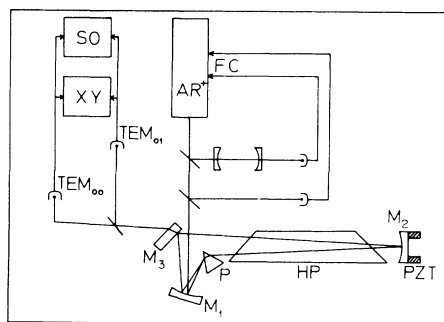


FIG. 1. Experimental setup. HP: Heat pipe; P: Brewster prism;  $M_1$ ,  $M_2$ : highly reflecting mirrors,  $r=200 \text{ mm}$ ;  $M_3$ :  $T=10\%$  plane mirror; PZT: piezoelectric transducer; SO: storage oscilloscope; XY:  $x$ - $y$  oscilloscope; FC: frequency control.

settings multimode operation occurred with irregularly varying output intensity. The modulation depth was 10% of the average power, which in turn was 25% of the maximum fundamental mode output power. The time average of the intensity distribution of a typical mode pattern for that situation is given in Fig. 2, showing the presence of several transverse modes. In Ref. 2, transverse mode structure has been shown to favor temporal instabilities, but no attempt was made to investigate the spatial variation of these instabilities.

For the measurements of the time-dependent intensity fast Si diodes were used as detectors. One of them was adjusted to the center of the  $TEM_{00}$  mode, while the other one was positioned at one of the maxima of the  $TEM_{01}$  mode (note that these two modes do not oscillate at the same resonator length). The diameter of the light-sensitive area of the diodes was only 15% of the diameter of the  $TEM_{00}$  mode to reduce integration over the beam cross section. The signals from the diodes were displayed on an  $x$ - $y$  oscilloscope and at the same time digitized to 8 bit at  $100 \times 10^6$  samples/sec with a storage oscilloscope. The sampled data were then transferred to a computer for evaluation.

Time traces taken simultaneously from the two diodes are shown in Fig. 3. Figure 3(a) corresponds to the diode at  $TEM_{00}$  maximum, and Fig. 3(b) gives the signal from the "TEM<sub>01</sub> diode". While there is some contribution from a fundamental frequency of about 8 and 16 MHz, respectively, which presumably stems from mode beating, both signals are irregular and clearly not identical.

Figure 4 shows the power spectra calculated from the time series using a 2048-point fast Fourier algorithm. Both spectra show the broadband noise characteristic for chaotic systems, but they differ in the distribution of the spectral density. The noise level of the detectors is  $-60$  dB.

The autocorrelation functions given in Fig. 5 for the two signals were calculated for 3000 points each. They are normalized to 1 for zero time delay. Again, some periodicity is obvious as it occurs in many chaotic systems. The fast decay of the envelope of the curve can be inter-

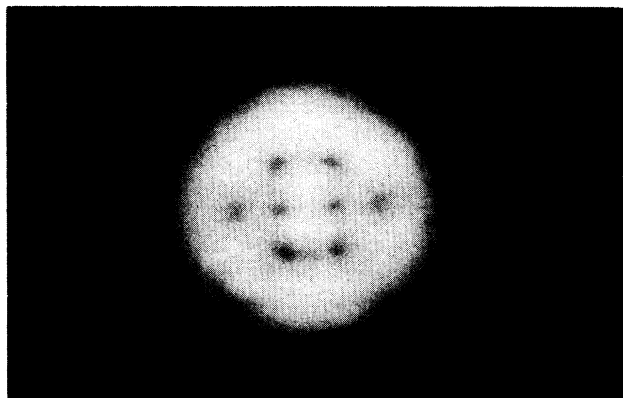


FIG. 2. Mode pattern for spatiotemporal chaotic multimode oscillation.

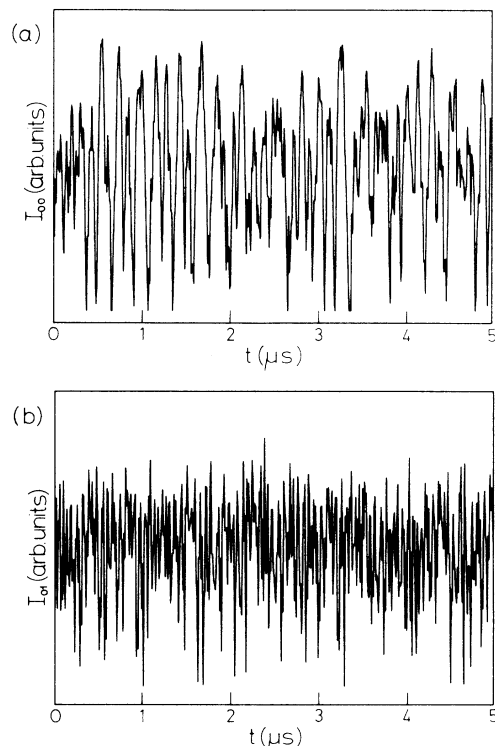


FIG. 3. Output intensity (arbitrary units, 8 bit) vs time for two different positions of the detector. (a) Center of  $TEM_{00}$  mode; (b) center of upper lobe of  $TEM_{01}$  mode.

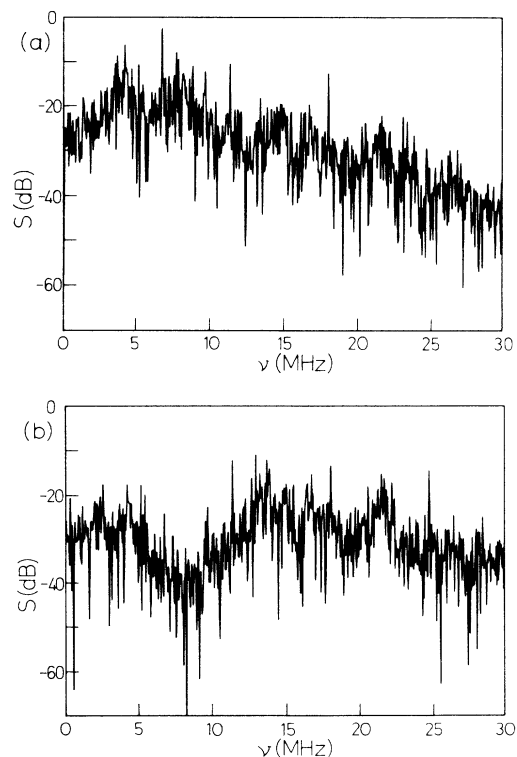


FIG. 4. Power spectra calculated from the intensity data given in Fig. 3.

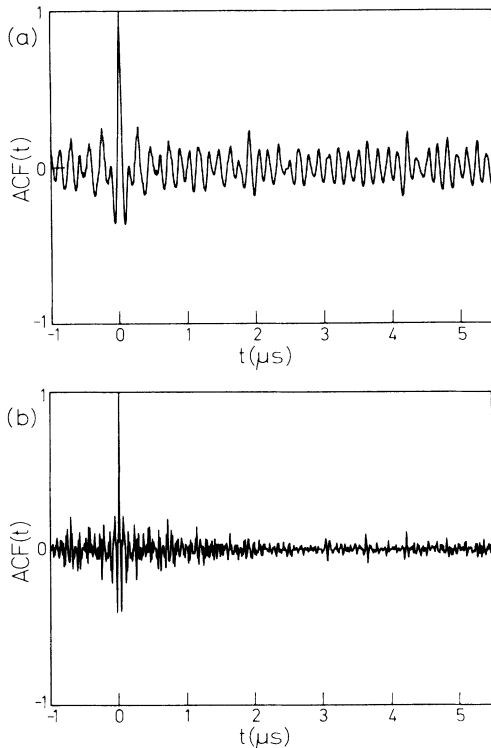


FIG. 5. Autocorrelation functions calculated from the intensity data. Note that the time scale starts with negative values.

interpreted as a consequence of chaotic behavior of the system. Note that these curves do not show the slow pulsation of the envelope known from other systems such as the Lorenz attractor. Note also that the time scale starts with negative values to allow for a phase shift between the two signals. In order to determine the relationship between the two signals their cross correlation function was computed using 3000 points. The result is given in Fig. 6. This plot is normalized to the geometric mean of the two autocorrelations for zero time delay.

We reconstructed for each of the time signals the underlying chaotic attractor and calculated its fractal di-

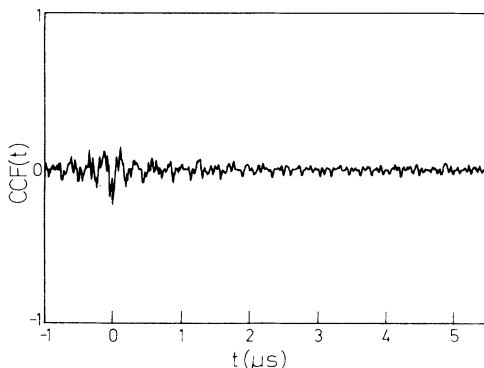


FIG. 6. Cross correlation function calculated from the intensity data.

mension from the correlation integral<sup>3</sup> using the maximum norm for embedding dimensions 1 through 15. The result is a fractal dimension of 3.9 for both signals within the uncertainties due to noise and the limited resolution. Plots of the correlation integral versus the box size  $r$  are given in Fig. 7, and the slope of these curves versus the box size is plotted in Fig. 8, showing the rapidly converging dimension values. For low values of  $r$  the curves show the usual influence of noise and limited resolution, while at high  $r$  values they are distorted when the boxes tend to cover the whole attractor.<sup>4</sup> Thus, we expect the correct fractal dimension to be given by the minimum value of the curves around  $r=20$ .

The intensity data measured at different points of the beam cross section show the same rapid decay of the autocorrelation function and give very similar results for the fractal dimension calculations. This points to the interpretation that they are different projections of only one spatiotemporal chaotic attractor. This is further shown in Fig. 9, which presents the  $x$ - $y$  representation of the two time signals as displayed by the  $x$ - $y$  oscilloscope. Note that due to the slow decay rate of the oscilloscope screen fluorescence the time interval displayed here is considerably longer (a few milliseconds) than the time needed to sample the digital data. The existence of well-defined trajectories during this time span, which is long compared to the decay time of the cross correlation function (see Fig. 6), clearly demonstrates a deterministic dependence between the two signals. The low value of the cross correlation function and its decay can result for different reasons.

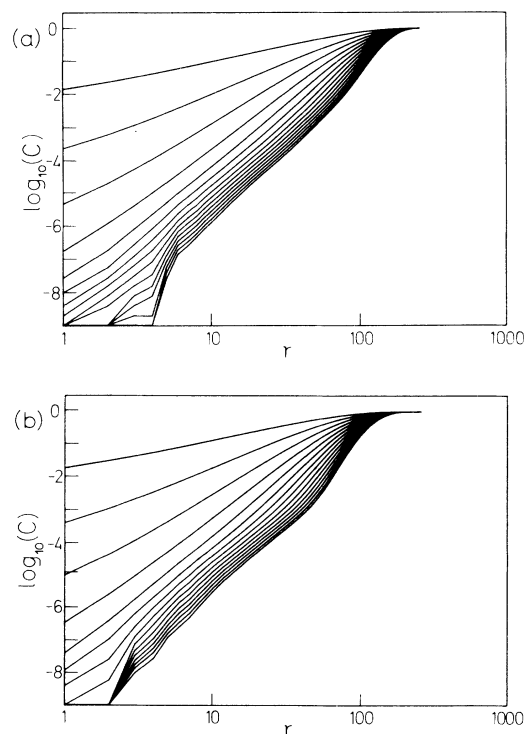


FIG. 7. Plots of the correlation integrals  $C(r)$  calculated from the intensity data vs  $r$ .

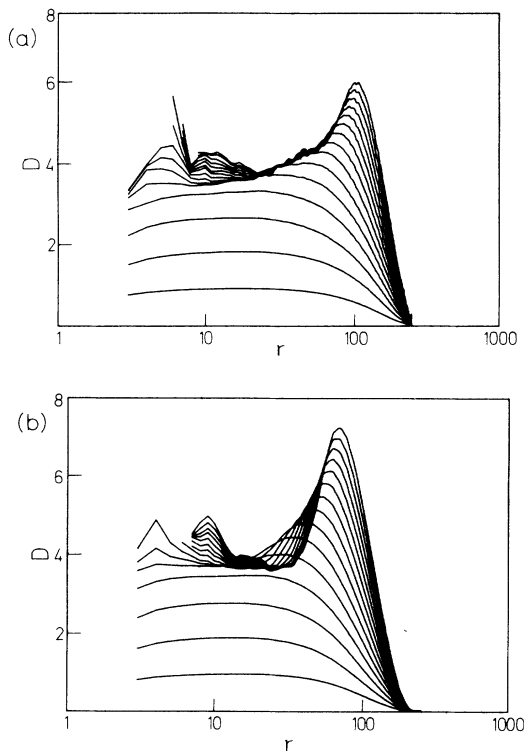


FIG. 8. Plots of the slopes of the curves given in Fig. 7 representing the fractal dimension vs  $r$ .

Noise can be ruled out since the spectral density of the measured intensity spectra is several orders of magnitude larger than the measurement system noise. In addition, the convergence of the fractal dimension values with increasing embedding dimension indicates that the random process is not noise but results from a low-dimensional attractor. A simple multimode emission where the laser would operate in a number of modes which do not interact with each other might also cause a low cross correlation. However, since such a multimode laser intensity spectrum would consist of discrete frequencies, the correlation would then reflect the superposition of several periods, at least in the form of "revivals," i.e., the envelope of the correlation function showing regularly spaced maxima and minima. This is not observed. We therefore conclude that the low correlation values are a consequence of the dynamic properties of the system: The modes are coupled and together establish a dynamical system which can be described by a single chaotic attractor. The low cross

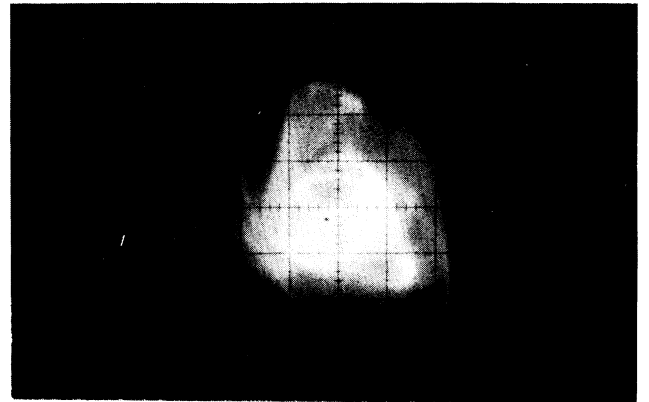


FIG. 9.  $x$ - $y$  representation of the two time signals as displayed by an oscilloscope.

correlation values then suggest the observed signals to be nearly orthogonal projections of this attractor.

The coupling between different transverse modes sensitively depends on their relative loss values, which in turn may be altered by changes in the resonator length. Also, different transverse modes are affected differently by the spatial variation of the pump field. This explains our observation that the instabilities occurred only for certain combinations of pump detuning and resonator length setting, although in optically pumped gas lasers a detuning of the pump can be compensated by a proper detuning of the laser via the Doppler effect.

Plots of data points sampled at time  $T$  versus points sampled at time  $T+t$  for either one of the intensity signals revealed no structure within the attractor for any delay  $t$ , in contrast to well-known lower-dimensional systems such as the Lorenz equations. This is probably due to the high fractal dimension of the attractor, since the increase of the dimension curves for large- $r$  values suggests the attractor to have some global structure (see Fig. 7).

In conclusion, we have observed a multimode instability in a  $\text{Na}_2$  ring laser that exhibits a spatial variation of the temporal behavior of the emitted intensity, which according to the analysis is chaotic: Time traces measured at two different locations in the beam cross section yield the same fractal dimension for the underlying attractor and the same decay rate for the autocorrelation function. They show only a small cross correlation. An  $x$ - $y$  representation of the two signals shows a deterministic dependence between them, indicating that they are governed by a single chaotic attractor.

<sup>1</sup>B. Wellegehausen, IEEE J. Quantum Electron. **QE-15**, 2108 (1979).

<sup>2</sup>R. Hauck, F. Hollinger, and H. Weber, Opt. Commun. **47**, 141 (1983).

<sup>3</sup>P. Grassberger and I. Procaccia, Phys. Rev. Lett. **50**, 346 (1983).

<sup>4</sup>M. Möller, W. Lange, F. Mitschke, N. B. Abraham, and U. Hübner (unpublished).

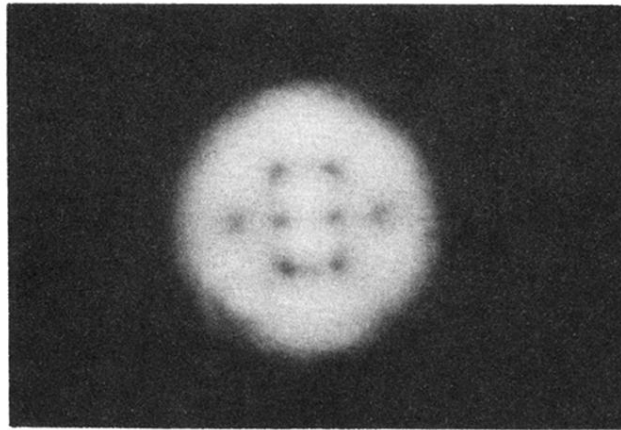


FIG. 2. Mode pattern for spatiotemporal chaotic multimode oscillation.

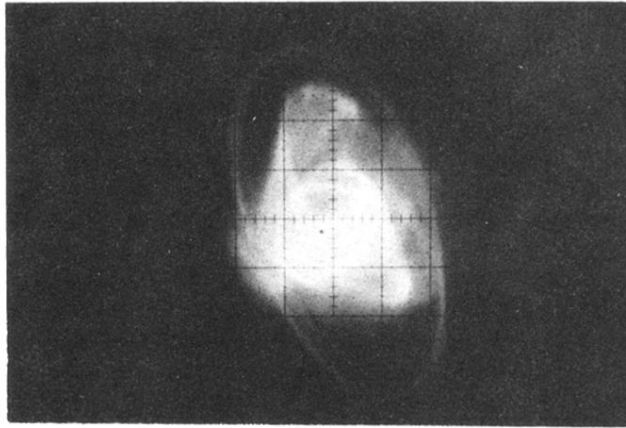


FIG. 9.  $x$ - $y$  representation of the two time signals as displayed by an oscilloscope.